2018

Multi-layer fast neutron detectors based on composite heavy-oxide scintillators for detection of illegal nuclear materials

Ryzhikov, V.D.; Naydenov, S.V.; Onyshchenko, G.M.; Piven, L.A.; Pochet, T.; Smith, C.F.

Elsevier

Ryzhikov, V. D., et al. "Multi-layer fast neutron detectors based on composite heavy-oxide scintillators for detection of illegal nuclear materials." Nuclear Instruments and Methods in Physics Research Section A: Accelerators, Spectrometers, Detectors and Associated Equipment 903 (2018): 287-296.
http://hdl.handle.net/10945/66347

Nuclear Inst. and Methods in Physics Research, A 903 (2018) 287–296

Contents lists available at ScienceDirect

Nuclear Inst. and Methods in Physics Research, A

journal homepage: www.elsevier.com/locate/nima

Multi-layer fast neutron detectors based on composite heavy-oxide scintillators for detection of illegal nuclear materials

V.D. Ryzhikov [a], S.V. Naydenov [b,*], G.M. Onyshchenko [a], L.A. Piven [a], T. Pochet [c], C.F. Smith [d]

[a] Institute for Scintillation Materials of the NAS of Ukraine, Kharkov, Ukraine
[b] Institute for Single Crystals of the NAS of Ukraine, Kharkov, Ukraine
[c] International Atomic Energy Agency (IAEA), Vienna, Austria
[d] Naval Postgraduate School, Monterey, CA, USA

ARTICLE INFO

Keywords:
Fast neutron detection
Inelastic and resonance neutron scattering
Radiation detectors
Multi-layer scintillator detectors
Nuclear safeguards
He-3 alternatives

ABSTRACT

We developed and characterized a new type (designated ZEBRA) of multi-layer composite heavy-oxide scintillator detectors for fast neutron detection for homeland security and nuclear safeguards applications. In this heterogeneous detector medium, composite layers comprised of micro-granules of heavy-oxide scintillators (ZWO, CWO, PWO, BGO, GSO(Ce), GOS(Ce) and others) dispersed in transparent plastic are alternated with layers of clear plastic that serve as scintillation light guides and as a neutron moderator material. The physical peculiarities of the neutron interactions and the principal mechanisms of fast neutron registration in these detectors are discussed in detail. The fast neutron intrinsic detection efficiencies and sensitivities of ZEBRA-detectors based on BGO, ZWO and GSO(Ce) composite scintillators in response to neutrons from ^{239}Pu–Be and ^{252}Cf sources were measured. These detectors had cross-sectional areas ranging from 16 to 100 cm^2. The sensitivities of such detectors of size $100 \times 100 \times 41$ mm^3 were found to be 40–51 cps/(nps × cm^{-2}), a level that is comparable to the sensitivity of a typical ^{3}He counter of 1600 cm^2 area. The intrinsic efficiencies and sensitivities of the ZEBRA-detectors also compare favorably with those of fast neutron detectors based on large-size heavy-oxide single crystals, but the multi-layer composite ZEBRA structures are much less expensive and can be easily manufactured in much larger dimensions. This work represents a significant advance from earlier single-crystal detector types as part of our effort to explore alternatives and improvements to conventional ^{3}He counters.

1. Introduction

One of the main challenges in nuclear security is the creation of detection systems for fast neutrons and mixed neutron/gamma radiation that would be highly efficient, compact, inexpensive, robust with respect to unfavorable conditions, and reliable in operation (see [1] and additional references therein). Reliable recognition of special nuclear materials (e.g., highly enriched Uranium and weapons grade Plutonium), and other neutron-emitting radioactive materials requires the creation of detectors with high detection efficiency for fast neutrons (intrinsic efficiency not less than 50%–60%). At the same time, practically all of the state-of-the-art detectors proposed for the replacement of ^{3}He counters due to the shortage of ^{3}He [2] can directly detect only slow and/or thermal neutrons, relying on the radiative capture reactions of light nuclei such as ^{6}Li or ^{10}B with high thermal neutron absorption cross-sections, but with relative insensitivity to fast neutrons. Many types of such neutron detectors have been proposed (see, for example, [3–9]). The probability of detection of fast neutrons with these detectors without using plastic moderators is orders of magnitude lower than for thermal neutrons, and the intrinsic efficiency of detection of fast neutrons therefore does not exceed a few percent. Even with massive moderators to moderate and thermalize the fast neutrons, the intrinsic efficiency of such systems for fast neutrons is ordinarily not higher than 10%–20%, and for ^{3}He detectors about 10%.

Traditionally, organic liquid and solid scintillators, including organic single crystals (anthracene, stilbene), and plastic scintillators have been used for detection of fast neutrons. Recently there were proposed composite capture-gated plastic detectors (see, for example, [10–13]) containing heavy nuclei such as ^{113}Cd, ^{155}Gd, ^{157}Gd with very high thermal neutron radiative capture cross-sections. Unfortunately, all these detectors have relatively low sensitivity to fast neutrons and intrinsic efficiencies not greater than 15%–20%. Moreover, plastic scintillators have high sensitivity to gamma radiation which interferes with and reduces sensitivity to fast neutrons.

* Corresponding author.
E-mail address: sergei.naydenov@gmail.com (S.V. Naydenov).

https://doi.org/10.1016/j.nima.2018.06.074
Received 1 September 2017; Received in revised form 24 June 2018; Accepted 25 June 2018
Available online 4 July 2018

At the same time, both actual experiments and numerical simulations of the interaction processes of fast neutrons passing through materials with heavy nuclei indicate that, alongside radiative capture (n,γ), for which cross sections are not sufficiently large in the relevant energy range, other interaction mechanisms – especially the reaction of inelastic scattering $(n,n'\gamma)$ of fast neutrons (see [14–19] and references therein) – can be used for improved fast neutron detection. It has been found [20–22] that promising materials for detectors keying on such interaction mechanisms are heavy-oxide scintillators which have relatively large cross-sections for inelastic scattering of fast neutrons on the heavy and medium nuclei of their component atoms, i.e., the nuclei Zn, Ge, Cd, Gd, W, Pb, Bi, etc. Such scintillators – $CdWO_4$ (CWO), $ZnWO_4$ (ZWO), $PbWO_4$ (PWO), $Bi_4Ge_3O_{12}$ (BGO), Gd_2SiO_5(Ce) (GSO(Ce)), etc. – were used in our previous work for the creation of novel single-crystal detectors of fast neutrons and mixed gamma-neutron fields [17–22].

In these scintillators the energy of fast neutrons is directly converted into the energy of gamma-quanta and/or conversion electrons, without relying on preliminary moderation of neutrons. In this case, the single-crystal scintillator plays a double role as an efficient converter of neutrons into secondary gamma-quanta and/or conversion electrons of intermediate energies (from some tens of keV to hundreds of keV), and as a scintillator that detects these internal gamma-quanta in either a counting or spectrometric mode. These detectors showed high intrinsic efficiency for detection of fast neutrons (in the range of 40%–50%) and high sensitivity (up to 24 cps/(nps × cm^{-2})) with compact scintillation assemblies using single crystals of dimensions ø40×80 mm coupled to 2-inch photomultipliers. This allows the use of such neutron detectors in compact stationary systems and portal monitors for detection of radioactive and fissionable nuclear materials [19]. Note that the primary application of the ZEBRA detectors envisioned in this paper is for pedestrian portal monitors rather than cargo monitors.

Our further studies [23–27] have also shown the possibility to create fast neutron detectors of comparable efficiency and sensitivity on the basis of a novel multi-layer composite scintillation structure that also relies on direct detection of fast neutrons through their interaction with scintillation materials of high effective atomic number ($Z_{eff} > 55$) and high density. We developed an original heterogeneous scintillation structure (brand ZEBRA), which is comprised of a series of alternating layers of two types – composite layers consisting of small particles of heavy-oxide crystalline scintillator material (CWO, ZWO, PWO, BGO, GSO(Ce), etc.) or ceramics (for example, Gd_2O_2S(Ce) (GOS(Ce)), etc.) embedded in an organic matrix (silicon rubber), and layers of an optically clear plastic material — polymethylmethacrylate (PMMA), polystyrene or others – to partially moderate incident fast neutrons while simultaneously serving as light guides for out put of the scintillation photons.

In detecting fast neutrons, such a detector medium utilizes, to the maximum extent, not just one, but several different channels of neutron interaction with heavy nuclei. In addition to direct detection of incoming fast neutrons that inelastically scatter in the composite layers, the structure also detects fast neutrons that have been elastically scattered within the moderator layers (while retaining kinetic energy above the inelastic energy threshold) and subsequently inelastically scatter in the composite layers. Additionally, fast neutrons with energies below the inelastic threshold provide an interaction signal from resonance and radiative capture of neutrons and elastic scattering in the hydrogenous material comprising the moderator/light guide layers. The detection of fast neutrons simultaneously over several different channels of interaction substantially increases the total intrinsic efficiency of detection.

It should be noted that similar exploratory research considering the transition from homogeneous (single-layer) to heterogeneous (i.e., dual-layer, three-layer and multi-layer designs of detectors) has also been considered elsewhere in several experimental and simulation efforts (see [28–30], etc.) to seek new, more efficient types of composite neutron detectors.

In this paper, we report our studies of the technical characteristics and the operating principles of a selected sample of our novel multi-layer neutron detectors (i.e., detectors of the ZEBRA-BGO, ZEBRA-ZWO and ZEBRA-GSO(Ce) types, having cross sectional areas ranging from 10 × 10 mm^2 to 100 × 100 mm^2), with the aim of understanding the physical reasons of their very high intrinsic efficiency in detection of fast neutrons, despite the much smaller volume of scintillator material (by more than a factor of ten) in these detectors as compared with detectors using heavy oxide single crystals.

2. Theoretical considerations

First consider the main interaction phenomena related to the incident flux of fast neutrons with a typical energy from 100 keV to 10 MeV (i.e., a range that is most representative of the sources of concern for security applications) with the constituent materials of the composite scintillator layer of the ZEBRA structure, considering only those possible neutron reactions which are most important with respect to fast neutron detection by the ZEBRA-detectors. Although there are other neutron reactions (including non-elastic processes apart from inelastic scattering and radiative capture, etc.), those mechanisms are of much lesser importance for these detectors and are not considered further here.

The types of interaction mechanisms of greatest importance include the following:

(i) inelastic scattering $(n,n'\gamma)$ (see, for example [31,32]) of fast neutrons on heavy and medium nuclei in the composite scintillator layers;
(ii) elastic scattering (n,n) [33] and deceleration (moderation) of neutrons of intermediate energies in the plastic layers of the detector;
(iii) elastic $(n,n)_{res}$ and non-elastic resonance interactions on heavy and medium nuclei in the composite scintillator layers, including resonance capture $(n,\gamma)_{res}$ of neutrons of resonance energies (from several tens of eV to tens of keV) in the scintillator layers after their moderation in plastic layers;
(iv) radiative capture $(n,\gamma)_{th}$ of neutrons reaching the range of thermal energies, which would be especially efficient for scintillators with odd neutron-capturing nuclei, such as ^{113}Cd, ^{155}Gd, ^{157}Gd, etc.

2.1. The role of inelastic scattering of fast neutrons

The main interaction of fast neutrons with energies E_n less than 10 MeV on heavy (atomic mass $A > 150$) and medium nuclei ($A > 50$) of the scintillators used in the ZEBRA structures is the inelastic scattering $(n,n'\gamma)$ reaction [31,32]:

$$A + n \rightarrow A^* + n' \rightarrow A + n' + (\gamma, \text{conversion}\, e^-), \quad (1)$$

where A is the target nucleus (Zn, Ge, Gd, W, Bi, etc.); n and n' are the incident and scattered neutrons with corresponding energies E_n and $E_{n'}$, for which $E_{n'} < E_{th} < E_n$, and energy E_{th} is the threshold of the reaction, i.e., the energy of the first excited level of the residual nucleus A^*. In Fig. 1, a scheme of inelastic neutron scattering is presented, with the possible generation of the following interaction products:

- The inelastically scattered neutron n' and its associated prompt gamma-quanta $(n,n'\gamma_1)$ from the de-excitation of the compound nucleus $(A+1,Z)^*$;
- Delayed (in the 0–30 μs range) gamma-quanta $(n,n'\gamma_2)$ from the de-excitation of the excited nucleus $(A,Z)^*$;
- Possible conversion electrons e_1 from the transfer of excess excitation $(A,Z)^*$ to the atomic orbitals of the final nucleus (A,Z) (for example, there is an internal conversion transition with 100% probability for the excited state of ^{155}Gd from its 121 keV energy level);

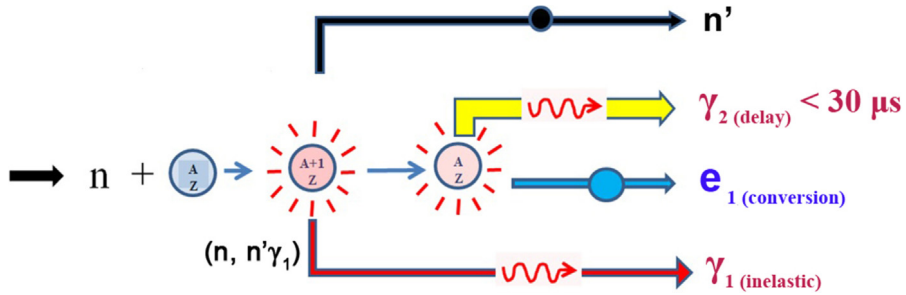

Fig. 1. Interaction products from inelastic scattering of fast neutrons with the heavy nuclei in the composite heavy oxide scintillator.

Neutron inelastic scattering $(n, n'\gamma)$ in heavy nuclei for neutron energies E_n up to 20 MeV occurs mainly through the formation of a compound nucleus [31,32]. At fast neutron energies starting from 5 to 6 MeV, the excitation energy U_{ex} of heavy nuclei falls into a continuum spectrum of the compound nucleus levels, which allows us to use the statistical model of the nucleus [31]. The excitation energy is the sum of the kinetic energy brought by the incident neutron to the nucleus, and the separation energy $S_n \approx 5.5$–6 MeV of the captured particle (neutron), which then is followed by the emission of the n' neutron from the compound nucleus. Within this model, the excitation energy U_{ex} of the compound nucleus is distributed onto the statistical fraction of the level spectrum, which determines the so-called nucleus temperature T. The nucleus temperature is evaluated from the excitation energy U_{ex} as $T \approx \sqrt{U^*/a}$, where $U^* = U_{ex} - S_n$, and the level density parameter $a \approx 10\,\mathrm{MeV}^{-1}$ for a nucleus with mass number $A \approx 150$. For nuclei with $A > 50$ the recoil energy $E_{recoil} \approx E_n/A \ll E_n$ is a very small value. Therefore, $U^* \approx E_n$.

Consider an incident neutron energy of about $E_n \approx 4$–5 MeV, i.e., on the order of the average energy of fast neutrons from a ^{239}Bu–Be source as used in our experiments. Then, for an excitation energy $U_{ex} \approx 5$ MeV, the nucleus temperature is $T \approx 0.7$ MeV. In the statistical model of nucleus, the average nucleon energy in the nucleus is $\overline{E} = 2T$ [31]. Therefore, the average kinetic energy $\overline{E}_{n'}$ of a neutron emitted from the compound nucleus is, in this case, approximately equal to $\overline{E}_{n'} \approx 2T = 1.4$ MeV. In the residual nucleus, the remaining excitation energy is 3.6 MeV. This corresponds to the excitation of several lower levels of the residual nucleus.

This excitation is removed, as a rule, by the emission of a series of accompanying gamma-quanta and/or conversion electrons. The relative output (on one scattering) of conversion electrons for such a nucleus as ^{155}Gd or ^{157}Gd may reach 30%–40%. For heavy nuclei, the energies of the secondary gamma-quanta are in the wide range from several tens of keV to several MeV. The conversion electron energy ranges over the energies of the inner K- and L- atomic shells. Their output is accompanied by characteristic soft X-rays and Auger electrons. The energies of the X-rays are in the range of 50–70 keV for heavy elements such as $_{64}$Gd or $_{74}$W and in the range 10–30 keV for medium elements such as $_{32}$Ge or $_{48}$Cd.

A peculiar feature of fast neutron inelastic scattering on heavy nuclei in the 2–10 MeV energy range is a rather significant (from 30% to 80%) energy loss as a result of this reaction. In the framework of above-mentioned statistical theory of nuclei, the emitted gamma-quanta obey a distribution of: $p(E_\gamma) \sim E_\gamma^3 \exp(-E_\gamma/T)$, with an average energy $\overline{E}_\gamma = 4T$, so $\overline{E}_{n'} \approx \overline{E}_\gamma/2$ after the first inelastic scattering; $\overline{E}_{n''} \approx \overline{E}_\gamma/2^2$ after the second scattering, and so on. Thus, the inelastically-scattered neutron has much lower energy than the incident neutron, and loses its energy in multiple inelastic scatters at an exponential rate. Because of this, fast neutrons of energies up to 10 MeV are subject to inelastic scattering an average of only once (or at most a few times [14]), after which their energy becomes lower than the threshold required for inelastic scattering. For many heavy nuclei, the energy threshold for inelastic scattering is about several hundred keV (see, for example, [34]). Below this threshold, the inelastic scattering channel is therefore closed, and such neutrons do not provide an inelastic scattering signal (i.e., they are not able to deposit their energy in a detector based on further inelastic scattering within the heavy oxide scintillator). Thus, when the scintillator thickness is increased, the recorded signal from inelastic scattering becomes saturated when such neutrons are detected. However, if the energy of these inelastically-scattered neutrons could be lowered even more (to resonance energies of 1–10 keV or to thermal energies below the cadmium threshold of 0.5 eV), an additional detection channel of resonance scattering and radiative capture would be opened. In this channel, alongside potential elastic scattering, the reactions of resonance scattering and radiative capture, as well as thermal radiative capture are also possible.

2.2. The role of elastic scattering and moderation of fast neutrons

The next important neutron reaction for ZEBRA detectors is elastic scattering, (n, n) [33]. In the thin heavy-oxide composite scintillator layers of the ZEBRA multi-layer media there is practically no deceleration of fast neutrons from elastic scattering reactions because the energy transfer from neutrons to heavy and middle mass nuclei (as well as to the oxygen nuclei of the silicon rubber) of the composite scintillator material is inversely proportional to the atomic number; on average, $\Delta E_n = 2E_nA/(A+1)^2 \approx E_n/A$ for $A \gg 1$, and, therefore, the energy loss on average does not exceed several percent of the neutron energy, $\Delta E_n \ll E_n$. Since the ZEBRA detector includes periodically alternating plastic layers, which contain large amounts of hydrogen with $A = 1$, the picture is substantially changed (i.e., $\Delta E_n \approx E_n/2$). For example, PMMA plastic contains about 53 atom percent hydrogen. Theoretical estimates show that 35–40 mm of the total thickness of the PMMA plastic layers is sufficient to moderate an initial neutron energy of 1–2 MeV to 1–2 keV. Moreover, moderation by each single plastic layer of 5 mm thickness results in a certain output of neutrons with energies below 10 keV (i.e., below the typical threshold energy for emergence of resonance neutron scattering on heavy nuclei in the composite scintillator layers). We emphasize here that the multi-layer design of the ZEBRA detector is better than a well-known double-layered design (i.e., one layer of scintillator plus one layer of moderator) or a three-layered design (i.e., a scintillator layer between two moderator layers), because the several separated scintillation layers can record more completely the total flux of all resonance neutrons — coming from deceleration of both the initial neutrons by elastic scattering in all of the plastic layers and the secondary neutrons formed by inelastic scattering in the outer scintillation layers.

2.3. The role of resonance and thermal neutron radiative capture

The second main mechanism of registration of neutrons by ZEBRA detectors is resonance capture $(n, \gamma)_{res}$ of moderated neutrons at resonance energies as well as radiative capture $(n, \gamma)_{th}$ of thermalized neutrons (a part of incident neutrons flux moderated down to thermal

energies) that may be described by the following equation:

$$(A, Z) + n \rightarrow (A + 1, Z)^* \rightarrow (A + 1, Z) + \gamma + \{\text{conversion } e^-\} \quad (2)$$

with the emission of prompt gamma-quanta from the transition from the excited levels of the compound nucleus $(A + 1, Z)^*$. In some cases (see Table 1) it is possible for there to be an internal conversion transfer from a low-energy level of an excited $(A + 1, Z)^*$ nucleus to a stable state $(A + 1, Z)$ with the emission of conversion electrons and delayed gamma-quanta, as well as a beta-decay of the excited parent nucleus $(A + 1, Z)^*$ into the ground $(A + 1, Z + 1)$ or excited $(A + 1, Z + 1)^*$ state of the daughter nucleus with the emission of high-energy electrons from beta-decay, delayed gamma quanta and/or conversion electrons and Auger electrons emitted from the transition of the excited nucleus $(A + 1, Z + 1)^*$ to the ground state.

All of these mentioned capture reactions may occur in the nuclei of the heavy-oxide scintillators. Note that certain nuclei have large cross-sections for such interactions (see Table 1). Resonance and thermal capture is accompanied by the emission of prompt and delayed gamma-quanta (and/or conversion electrons with characteristic X-rays radiation) in a broad energy range. Thus, the recording of this secondary radiation can substantially increase the fast neutron detection efficiency.

Note that the resonance neutron cross-sections (mostly due to radiative capture) for the identified heavy and middle mass nuclei are not generally less than the characteristic cross-sections for inelastic scattering of neutrons, and sometimes they are even much larger. Comparative values of microscopic radiative capture cross-sections, based on the JENDL nuclear data base [34], are presented in Table 1. They include cross-section data for radiative capture σ_{th} (in the energy range from 0.0253 eV to 0.5 eV), resonance scattering σ_{res} with gamma-quanta escape (the resonance integral covers the energy range from 0.5 eV to 10 MeV), and inelastic scattering σ_{in} (for a fixed fast neutron energy of 14 MeV, representative because this value tends to remain fairly constant over a considerable energy range) on natural nuclei that are constituents of our heavy oxide scintillators comprised of BGO, ZWO, GSO(Ce), CWO or PWO.

The resonance integral for the resonance capture cross-section of such nuclei as ^{184}W or ^{155,157}Gd can reach hundreds of barns (see Table 1). Therefore, for recording of resonance neutrons, a sufficient thickness of composite scintillators like ZWO or GSO(Ce) should not exceed 1 mm. Thus, with additional detection of resonance neutrons, the detection efficiency is increased, even though the total thickness of the active layers of heavy oxide composite scintillators in our heterogeneous detectors is much smaller than the thickness of a single crystal scintillator made of the same material (used in a conventional neutron detector with comparable efficiency).

Analysis of data from Table 1 shows that promising scintillators for the production of multi-layer ZEBRA-detectors might be composite materials based on: (i) BGO, due primarily to resonance neutron capture and inelastic scattering on the stable nuclei ^{70}Ge, ^{74}Ge, ^{76}Ge and the large internal conversion potential for the excited nuclei ^{71}Ge*, ^{73}Ge* (inelastic scattering), and ^{75}Ge*; (ii) ZWO due to resonance capture on all the stable nuclei ^{182}W, ^{183}W, ^{184}W, ^{186}W and internal conversion on excited ^{183}W* (inelastic scattering), ^{185}W*, ^{187}W*; and (iii) GSO(Ce) due to the huge resonance capture and internal conversion electron emission for the stable and excited nuclei ^{155}Gd, ^{157}Gd, respectively.

3. Design and operating principles of multi-layer ZEBRA-detectors

3.1. Design and peculiarities of multi-layer ZEBRA-detectors

In our previous work [23–27], we proposed and tested a new design (Fig. 2) of the multi-layer composite scintillation detector, which could detect mixed neutron and gamma radiation. The ZEBRA detector (see photo in Fig. 3) consists of alternating and optically connected (i.e., glued) parallel planar layers of two types: (1) 5–6 plates (films) of the comprised of granules of scintillator material dispersed in a transparent organic matrix (rubber glue), with a thickness of ~1–2 mm; and (2) 7–8 plates of a transparent plastic, with a thickness of ~5–7 mm, which act both as a moderator for neutrons and as a light guide for collection and transport of the scintillation photons.

The first layer type (i.e., the thin layers containing the dispersed heavy scintillator particles) required a transparent organic glue-like material with low-molecular weight and thermal shock resistance. For this layer type, we used SKTN-B™, a synthetic rubber material with a refractive index of $n_{glue} = 1.42$. The average size of the heavy-oxide crystalline scintillator fragment in these composite scintillator layers was about 150–200 μm. The overall concentration of the small crystalline fragments (granules) was chosen such that the volume fraction of the active scintillator in the composite material was not less than 60%–70%.

For the second layer type (i.e., the thicker light guides), the transparent optical plastic polymethylmethacrylate (PMMA) with a refractive index of $n = 1.49$ (at light wavelength of 540 nm) and an absorption coefficient of $\alpha = 0.03\,\text{cm}^{-1}$ was used.

The outer surface of the detector is covered with a diffuse light-reflecting coating (except at the one end that is attached to the light receiving device to provide optical contact and spectral matching). As an outer coating, a polytetrafluoroethylene (PTFE) membrane with a diffuse reflectivity coefficient of about 98% was used. The external reflector is very important for good light collection and high detection efficiency. An internal reflector as shown in Fig. 2 (i.e., an aluminized Mylar film in the middle of the composite layers) was considered but was found not to be essential and is therefore omitted in some of the detector variants tested. Although it provides a small increase in the scintillation output, it introduced production difficulties that did not justify the small improvement in performance. Nevertheless, we tested detectors of both types. The tested detectors without this internal reflector in the composite layers were found to have detection efficiencies approximately the same as those with reflectors.

It was experimentally found that a high intrinsic detection efficiency of fast neutrons (up to 40%–50%) required that the full thickness of the multi-layer detector be just 40 mm. This dimension is comparable to the diameter of the large heavy oxide single-crystal homogeneous neutron detectors we have previously developed and tested [19].

We prepared and tested a set of ZEBRA-detectors of large size ($100 \times 100 \times 41$ mm^3) on the basis of different scintillators — BGO, ZWO and GSO(Ce). Each detector had 6 composite layers of thickness 1 mm and 7 layers of transparent plastic with thickness 5 mm (Fig. 3). The sensitive detector area under irradiation by neutron flux from the side (i.e., in the direction transverse to the plates) was 100 cm^2. In the general case, the multi-layer detector can be comprised of an arbitrary number of plates, without any limitations on their area or the total detector thickness.

For the transparent light-guide layers, we also considered using a scintillating plastic transparent material. We tested both types of such detector configurations. The neutron detection efficiency for the detectors incorporating scintillating plastic as the light-guide material was determined to be better, but the neutron/gamma rejection ratio was not as good. It is expected also that the production cost of this alternate configuration would be somewhat higher. Further research and development of the ZEBRA-detectors with scintillating plastics is anticipated to be included in our future work.

The main difference between ZEBRA-detectors and well-known conventional "capture-gated detectors" [10–13] is that the latter are loaded by materials with "capture-gated" nuclei (such as ^{113}Cd, ^{155}Gd, ^{157}Gd) with very large thermal neutron radiative capture cross-sections only for detection of thermal neutrons. In contrast, ZEBRA detectors include layers of composite heavy oxide scintillators with "heavy" (Bi, W, Gd, others) and/or "medium" atomic mass (Ge, Zn, Cd) nuclei with high probabilities of both fast-neutron (above about ~1 MeV) inelastic scattering and resonance neutron interactions (mainly, resonance capture with gamma quanta and conversion electron emission) in an

Table 1
Neutron interaction parameters for key nuclei in heavy oxide scintillators. Average cross-sections for neutron interactions with nuclei (mixtures of natural isotopes) based on data from [34]. Internal conversion electron emission (with relative intensity more than 10% for a single interaction) and beta-decay data (with decay half-lives) are taken from [35]. Cross-section values are given in barns (1 barn is equal to 10^{-24} cm^2).

Nuclei/ atomic number	σ_{th}	σ_{res}	σ_{in}	Conversion electrons from (n,γ), $(n,n'\gamma)$ reactions	Fastest beta-decay nuclei in (n,γ) reaction
$_{30}$Zn	1.063	2.539	0.619	–	^{69}Zn, 56.4 m
$_{32}$Ge	2.218	5.997	0.566	^{71,73,75,77}Ge*	^{77}Ge*, 52.9 s
$_{48}$Cd	3.294×10^3	6.659×10^1	0.416	^{111}Cd*	^{117}Cd, 2.49 h
$_{64}$Gd	4.119×10^4	4.011×10^2	0.652	^{155,157,159,161}Gd*	^{161}Gd, 3.66 m
$_{74}$W	1.819×10^1	3.551×10^2	0.428	^{183,185,187}W*	^{187}W, 24.00 h
$_{82}$Pb	0.154	0.142	0.324	^{206,207}Pb*	^{209}Pb, 3.23 h
$_{83}$Bi	0.342	0.172	0.361	–	^{210}Bi, 5.01 d

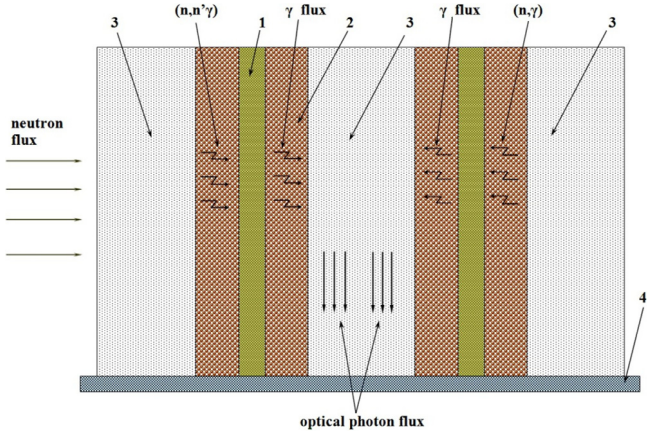

Fig. 2. Design and function of the multi-layered composite detector (only several layers are shown, and the layer thicknesses are not to scale): 1 — internal reflector made of aluminized Mylar (it is absent in many ZEBRA detectors variations); 2 — active layer of composite scintillator material; 3 — passive layer of light-conducting plastic; 4 — photoreceiver (PMT or Si-PM).

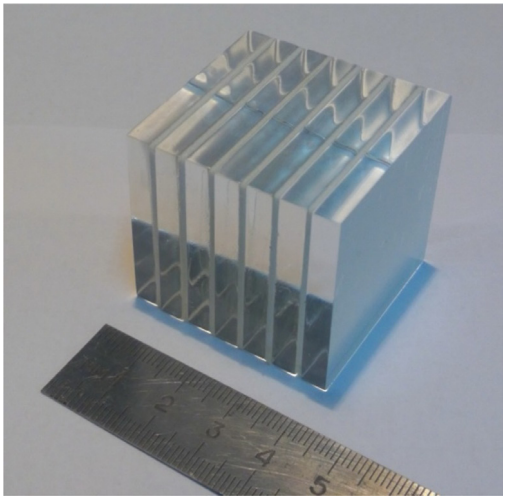

Fig. 3. Photo of a typical ZEBRA-detector on the basis of the heavy-oxide composite scintillator ZWO with dimensions 40 × 40 × 41 mm.

intermediate energy range from 10s of eV to 10s of keV. In addition to inelastic scattering, the resonance neutron interaction (capture) reaction is a key reaction for operation of ZEBRA-detectors.

The ZEBRA detectors are designed for the direct detection of fast neutrons and for the discovery of small quantities of transuranic elements (by also detecting the accompanying gamma-radiation). Detectors of this type are characterized by the following features:

(i) it is possible to prepare detectors of arbitrarily large working area of the detecting plates, which allows a substantial (by many times) increase in the sensitivity of such detectors in comparison with detectors based on inorganic single crystals;
(ii) the preparation of large area layers of composite scintillators (on the basis of small-crystalline fractions of broken crystal fragments or micro-crystalline powders obtained by solid-phase synthesis) is much simpler and less expensive than the growth of costly large-sized single crystals, the maximum size of which is essentially limited by the growth technology;
(iii) within the framework of a multi-layer design for such detectors, engineering combinations using different scintillation materials are possible, aiming at optimization of its productivity for different tasks.

3.2. The principle of operation of multi-layer ZEBRA-detectors

The principle of operation of ZEBRA detectors is as follows. The incident neutron flux interacts with the active layers of the composite heavy-oxide scintillator and plastic. The composite scintillator layers contain heavy nuclei with high cross sections for both inelastic scattering and radiative capture in the region of resonance neutron scattering (the energy of epithermal and intermediate neutrons). The alternating transparent plastic layers serve as a moderator of fast neutrons (slowing them down from fast energies to epithermal/intermediate energies) and simultaneously as optical light guides through which the scintillation light transmitted. Fast neutrons interact directly with the layers of the composite scintillator through an inelastic scattering reaction if their energy is high enough for this (i.e., exceeding the energy threshold for inelastic neutron scattering (usually at least several hundred keV)). Additionally, incident neutrons also interact with the heavy nuclei of the composite scintillator material as a result of the resonance scattering reaction if their energy falls into the appropriate energy interval after moderation in the plastic layers. The moderation of the incident neutrons mainly occurs in the "thick" layers of hydrogen-containing plastic as a result of the elastic neutron scattering reaction. Elastic neutron scattering inside the "thin" layers of the composite can be neglected, since the volume fraction of the organic filler is small, and the energy loss due to scattering in the heavy oxide scintillator granules is inversely proportional to the atomic mass of the heavy nuclei ($\Delta E_n \propto E_n/A \ll E_n$ if $A \gg 1$). Following elastic scattering in the transparent plastic layers, moderated neutrons will move in any direction, so most of them will reach the composite scintillator layers except the small fraction that are scattered outward in the two outer plastic layers.

A feature of the ZEBRA detector is that the composite scintillator material consists of heavy nuclei with a large value of the resonance integral for the reaction $(n,\gamma)_{res}$ and/or concomitant resonance capture reactions with emission of conversion electrons. If the value σ_{res} reaches several hundred barns (e.g., W, Gd, see Table 1), then it can be shown that each neutron slowed down to the resonance energy region is highly likely to be absorbed and recorded as a secondary gamma quantum in a rather small volume of the scintillator of thickness of several hundred microns. Consequently, with high probability, fast neutrons moderated to resonance energies may be registered in each layer of the composite scintillator.

As a result of the reactions $(n, n'\gamma)$ and $(n, \gamma)_{res}$ gamma quanta are produced in the thin composite layers in the energy range of 5–300 keV, an energy range that allows their signal to be efficiently detected following collection and transport to the photodetector. Gamma rays emitted in one active layer can be registered both in the same and in several adjacent layers of the heavy-oxide composite scintillator. Because of the relatively small thickness of the transparent plastic layers (as well as its low effective atomic number and density), there is no significant attenuation of the secondary gamma radiation in them. The most likely energy of gammas released by inelastic neutron scattering is from 10s of keV to 100s of keV. The energies of gammas from resonance neutron capture (and/or energy of conversion electrons by accompanying reactions) are mainly about 10s of keV, although they may reach 100s of keV or even MeVs for some nuclei. The most probable interaction of gammas with the heavy-oxide composite scintillator is the photo-effect because the energy of these gammas lies mainly in the range below 300 keV as indicated by our experiments.

The scintillation light obtained by the interaction of the secondary gamma quanta (and/or conversion electrons) with the scintillator material first passes from the composite layer to the transparent plastic layer, and is then transmitted to the photodetector (see Fig. 2). The geometry of the layers and the optical parameters of the multi-layer detectors (including the optical and spectral correspondence of the scintillator and light-guide layers, the interface to the photodetector, the characteristics related to total internal reflection and Fresnel losses and the optical transparency of the composite scintillator and transparent plastic media, etc.) have been chosen specifically to optimize the light output.

Due to its special design, ZEBRA-detectors have 2–3 times lower gamma ray sensitivity in comparison to their neutron sensitivity (per incident particle with the same energy). That is one of the achievements of fast neutron detectors based on multi-layer heavy-oxide scintillators in comparison with those based on organic (plastic) scintillators. For fast neutron detection against background gamma radiation, high-energy external gamma rays are rejected by the choice of a special spectrometry range below of 300 keV as previously proposed in our fast neutron detection method (see references [17–20]). Lower energy gamma rays from background are rejected by external filters and detector calibration (i.e., the use of initial and/or real-time special algorithms and software designed for neutron portal monitors based on our detectors). Moreover, Compton gamma rays may be rejected by special separation methods including those developed previously and referred to as the "spectrometry windows" method [20].

Unlike a homogeneous single-crystal detector, in a heterogeneous detector such as the ZEBRA system, neutrons are detected by each active layer with a sensitive area equal to the cross-sectional area of the detector. Each active layer plays the role of an "internal" neutron mono-detector. In fact, neutrons are simultaneously recorded not by one but several such "internal" mono-detectors. The total area of all internal active layers will be higher than the sensitive area of the detector itself. Therefore, the sensitivity of the multilayer detector as a whole increases substantially, as indicated in our experiments. With a total active-layer thickness of 6–7 mm, the detection sensitivity of fast neutrons by a multilayer ZEBRA-detector is comparable to the sensitivity of a single-crystal scintillation detector in which the scintillator layer is ten times thicker in the direction of transmission (this is further discussed in Section 5).

4. Method of fast neutron measurements and gamma shielding geometry

We have carried out studies of intrinsic detection efficiency and sensitivity of the prepared ZEBRA-detectors under irradiation by ^{239}Bu–Be and ^{252}Cf fast neutron sources. For these detectors, a large volume and a large sensitive area are characteristic features. This requires substantial changes in the procedures and geometry of measurements as compared with our previous studies on neutron detection carried out for compact single crystals. In particular, we had to substantially increase (up to 100 cm) the distance from the source to the detector to preserve the geometry of a narrow (parallel) neutron beam falling on the detector, to avoid the effects of broad beam geometry and the related edge effects, corrections, etc. Also, in detecting fast neutrons against the background of accompanying gamma-radiation from one and the same source, one has to use shielding filters (as a rule, shields are made of lead or iron with a thickness of up to 40–50 mm) for suppression of low and medium energy gamma-quanta. In the filter material, as well as in the objects surrounding the source and the detector (concrete walls, construction elements, parts of experimental installation, etc.), scattered radiation may appear due to elastic and inelastic scattering of the fast neutron flux. Also, this stray emission can accumulate with time if long-lived nuclides are formed in interaction reactions with fast neutrons. This scattered radiation can distort the results of fast neutron detection by tens of percent or more.

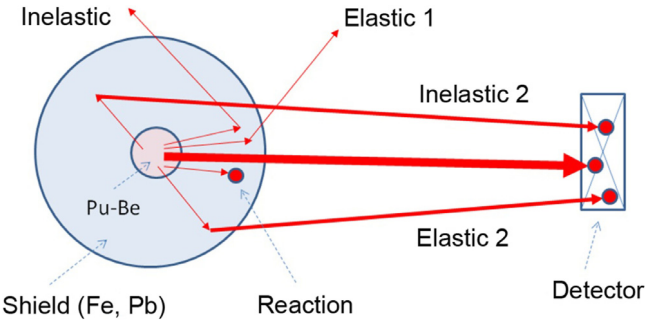

Fig. 4. Detection of fast neutrons in spherical geometry. Compensation is required for narrow neutron beams primarily scattered in the source shield either out of (re-scattered beams "Elastic 1" and "Inelastic 1") or into (re-scattered beams "Elastic 2" and "Inelastic 2") the neutron flow directed toward the detector.

An efficient compensation of scattered radiation can be obtained if the measurements are carried out not in planar, but in spherical geometry [36], using filters that fully surround the source and/or the detector (Fig. 4).

If the substance of which the shielding is made (in the form of an ideal sphere of radius R) can mainly scatter neutrons, but practically does not absorb them (e.g., an iron or lead sphere), the number of neutrons coming out of the sphere will not change along any direction from the source to detector (due to spherical symmetry), so the neutron current will be unchanged in any point of the detector. Scattering of neutrons, i.e., their escape from the narrow beam directed to the detector, in certain points of the spherical layer is compensated by scattering of neutrons (with their "joining" the beam) in other points. The resulting neutron flux onto a finite-sized detector will be also unchanged. An important condition for this is the isotropic character of the radiation source. Otherwise, after scattering, the angular distribution of the radiation will be changed, and, consequently, the beam falling onto the detector will also be changed (in contrast to the situation of an unshielded source). However, if the distance between the source and detector is sufficiently large (e.g., $r > 4R$), the isotropic character of the radiation is preserved, and the inverse square law $I(r) \propto I_0/r^2$ for the flux intensity at the distance r from the source is not violated. If we neglect also the dependence of intrinsic detector efficiency upon neutron energy, $\varepsilon(E) \approx \varepsilon = \text{const}$, the counting rate V of the detector, if spherical shielding from gamma-quanta is used, can change only because of possible absorption of neutrons in the shielding material. The appropriate correction, which is the same for all measurements, is determined with an error of less than several percent. It is equal to:

$$\text{spherical shield}: \quad V \to k_c V; \quad k_c = \frac{V^*}{V_0^*} = \exp\left(-n\sigma_a d_{sph}\right), \tag{3}$$

where k_c is the correction coefficient for the case when spherical shielding is present, n is the concentration of heavy nuclei in the shielding

material, σ_a is the absorption cross-section of fast neutrons and d_{sph} is the thickness of spherical layer. Readings of calibration measurements with a test detector with and without shielding are denoted as V^* and V_0^*, respectively.

Let us carry out calculations according to (3), e.g., for lead shielding with a spherical layer of 4 cm thickness. The concentration of nuclei $n = N_A\,\rho/M$, where $N_A = 6.023\times10^{23}$ mol^{-1} is the Avogadro number, ρ is the density of shielding material and M is the molar (atomic) mass. For lead, the molar mass is 208 g mol^{-1}, the density is 11.3 g cm^{-3}, the neutron absorption cross-section averaged over the energy spectrum of ^{235}U fission is $\sigma_a = 0.0024$ barn, whence $k_c \approx 0.97$, i.e., losses of the full neutron beam in the shielding are about 3%. For other spectra of fast neutron energies, these losses are typically smaller. Thus, in lead the capture cross-section of neutrons for 14 MeV energy is 0.00011 barn, which gives neutron losses in the gamma shielding not exceeding 0.14%.

The multiple elastic scattering of neutrons in the shielding substantially distorts the simple expression (3), since multiple changes in neutron direction would violate the spherical symmetry of the distribution of scattered beams, and the advantages of the spherical geometry of irradiation are lost. However, elastic neutron scattering cross-sections are not large for heavy nuclei such as iron and lead in contrast to light nuclei (in lead, the mean free path reaches 15 cm at a neutron energy of 4 MeV). This makes it possible to use spherical shielding of large thickness, which will be sufficient for full absorption and discrimination of gamma-quanta emitted by the source up to energies of several MeV.

According to our method of fast neutron detection using heavy oxide single crystals and multi-layer composite scintillators, neutrons are detected mostly by gamma-radiation that is emitted by scintillator nuclei in the reactions $(n,n'\gamma)$ and $(n,\gamma)_{res}$. To suppress the accompanying gamma-radiation from the neutron source, we prepared a filter in the form of a lead sphere with an outer diameter 100 mm, a spherical shell of thickness 40 mm and an internal well to place the source in the center of the sphere. To exclude the effects of external high energy gamma-quanta upon detector readings, we chose the spectrometric range of gamma-quanta detection as 20–1000 keV. For a quantitative account of the effects of spherical shielding on measurements, it is sufficient to measure the counting rate with and without a filter by a detector with calibrated efficiency. We used a detector based on a ^{6}LiI(Eu) scintillator of dimensions ø15×10 mm. It was found that for a ^{239}Bu–Be source inside the said lead sphere, the neutron flux is weakened by not more than 3%–4%.

For scintillators of small volume (1–10 cm^3) the differences in measured intrinsic neutron detection efficiency for cases of planar or spherical shielding from the source gamma-quanta are not significant. For detectors of larger size, better results are obtained with measurements in spherical geometry, when the scattered radiation in the shielding is compensated better (see the previous section).

5. Experimental results and discussion

5.1. Experimental setup

Based on our studies, we developed an experimental scheme (Fig. 5) and prepared an experimental board for recording fast neutrons by single crystal and multi-layer ZEBRA-detectors of different sizes. The neutron flux density at the detector location was determined according to the reference data of the source. Two different sources were used in our measurements:

- ^{239}Bu–Be isotropic source, with average neutron energy 4.5 MeV, output neutron flux 1.06×10^5 neutron/s and flux density 0.76 neutron/(s cm^2) at r = 100 cm from the source; source dimensions were ø20 × 30 mm;
- ^{252}Cf source with average fast neutron energy 2.13 MeV, activity 20×10^6 Bq, output neutron flux 2.35×10^6 neutron/s and flux density 2.34 neutron/(s cm^2) at r = 100 cm from the source.

The neutron spectra of the ^{239}Bu–Be and ^{252}Cf sources are different (see, for example, [37]). In the first case, it is a characteristic spectrum of the nuclear reaction $^9\mathrm{Be}\,(\alpha,n)^{12}\,\mathrm{C}$ due to capture of alpha-particles formed as a result of ^{239}Pu decay. In the second case it is a spectrum of spontaneous fission neutrons. However, after passing through the spherical lead shielding, the transformed neutron spectrum also resembles the fission neutron spectrum. Therefore, the measurements of parameters of fast neutron detectors (detection efficiency and sensitivity) using both sources can be considered equivalent in the spherical geometry.

5.2. Neutron detection efficiency and sensitivity of new fast neutron detectors

Within the experimental framework (Fig. 5), we carried out a set of measurements for detection of fast neutrons by heavy oxide single crystal and multi-layer composite scintillators, including measurements of the spectrometric response of these detectors to spectra of gamma-quanta emitted in nuclear reactions of fast neutrons with heavy scintillator nuclei and measurements of neutron detection efficiency. This intrinsic efficiency is defined as ratio $\varepsilon = N_{reg}/N$, i.e., the ratio of the number of registered neutrons to the total number of neutrons entering the detector during a specified time interval.

In the spectrometric mode, cutting out the working energy range from the detector's output spectrum and summing up the number of recorded pulses, we can determine the counting rate V for pulses of all recorded neutrons, as well as counting rate V_0 without the source. The counting rate can also be measured in the counting mode. As can be seen from our measurements, the intrinsic detection efficiency in the counting mode is about 30% higher than in the spectrometric mode with the window $E_\gamma = 5-300$ keV (i.e., not all of the pulses from the reactions of neutrons with scintillator material are recorded in the spectrometric mode). After calibration of the detecting system, we obtain the detection efficiency as:

$$\varepsilon = k_c\left(\frac{V-V_0}{F-F_0}\right), \tag{4}$$

where k_c is the calibration coefficient (3) in the case when shielding from gamma-quanta is present; F and F_0 are neutron fluxes from the source and in the absence of source (background), respectively, at the point of recording by the detector. This efficiency is normally expressed as a percent.

The sensitivity η is defined as the ratio of the counting rate of the useful signal to the flux density of the incident neutrons:

$$\eta = \frac{(V-V_0)}{(I-I_0)}, \tag{5}$$

where I — neutron flux density of source and I_0 — neutron flux density of background. The sensitivity is expressed in area units, $[\eta] = \mathrm{cps}/\left(\mathrm{nps}\times\mathrm{cm}^{-2}\right) = \left[\mathrm{cm}^2\right]$. Within the geometric framework of planar parallel "narrow beams", the following relationship can be obtained:

$$\eta \approx \varepsilon\, S_{eff}, \tag{6}$$

where we introduce the effective area $S_{eff} = S_{det}\,\langle\cos\psi\rangle$ of the total sensitive surface of the detector; S_{det} is the apparent area of the detector surface in the direction of irradiation; $\langle\cos\psi\rangle$ is the average value of the cosine of angle between the normal surface and the direction of irradiation. For scintillators of rectangular shape, S_{eff} coincides with the area of their side surface in the direction of irradiation (normal to the surface). Therefore, for a cubic single crystal of dimensions 10 × 10 × 10 mm^3, the detector sensitivity is $\eta = \varepsilon \times 1\,\mathrm{cm}^2$. For scintillators of cylindrical shape $D \times H$ with irradiation onto the circular end face, S_{eff} coincides with the area of the cylinder cross-section $S_{eff} = \pi D^2/4$, and under irradiation onto the side normal to the cylinder axis $S_{eff} = (2/\pi)\,DH \approx 0.64\,DH$. For single crystals of dimensions ø40 × 80 mm under side irradiation $\eta \approx \varepsilon\times20.37\,\mathrm{cm}^2$. For multi-layer ZEBRA detectors of dimensions 40 × 40 × 41 mm, 100 × 40 × 41 mm and 100 × 100

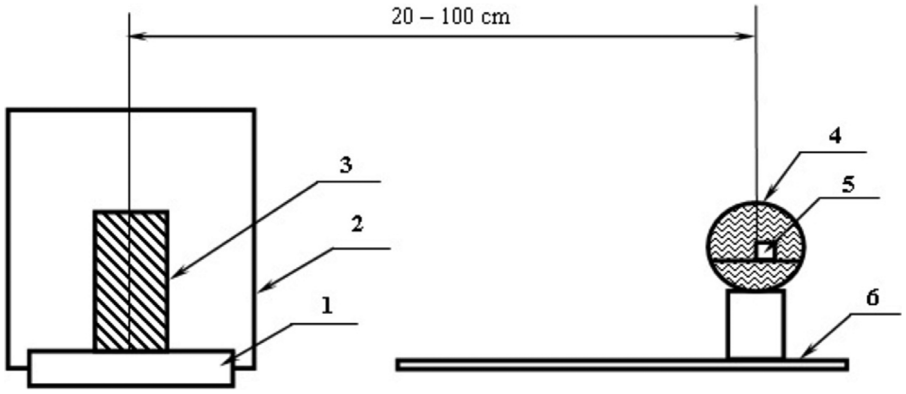

Fig. 5. Experimental set-up for the measurement of fast neutron detection efficiency in a direct spherical geometry of the source with shielding from gamma-quanta: 1 — photoreceiver (2′ or 3″ Hamamatsu R1307 PMT and 5" ET Enterprises Limited 9390 KB PMT in correspondence with the different sizes of scintillation detectors from 10 × 10 × 10 mm^3 up to 100 × 100 × 41 mm^3 volume), 2 — light protective housing, 3 — detector under study, 4 — lead sphere, 5 — neutron source, 6 — supporting surface with source movement mechanism and scale bar.

× 41 mm under irradiation normal to the plates the sensitivities are $\eta \approx \varepsilon \times 16\,\mathrm{cm}^2$, $\eta \approx \varepsilon \times 40\,\mathrm{cm}^2$ and $\eta \approx \varepsilon \times 10^2\,\mathrm{cm}^2$, respectively.

In Table 2 we present, for comparison, the measured fast neutron intrinsic detection efficiency and sensitivity for single crystal and multi-layer composite heavy-oxide scintillators comprised of ZWO, BGO and GSO(Ce). The measurements for the multi-layer ZEBRA-detectors were carried out using composite scintillators comprised of ZWO, BGO and GSO(Ce), with the same number and thicknesses of the layers (i.e., with the same total thickness of the detector), but with different sensitive (cross-sectional) areas. The measurements were carried out in conditions of broad beam and spherical geometry accounting for corrections for natural background. However, the experimental installation was placed in a closed space, and near the detector and neutron source there were elements of metal construction, laboratory furniture, concrete walls etc., so, there was high potential for accumulation of scattered radiation from reactions of fast neutrons $(n, n'\gamma)$ (iron) and (n, γ) (concrete, etc.), as well as from scattered gamma radiation emitted by the neutron sources and scattered by external metal and concrete materials. We measured the intrinsic detection efficiency (Table 2) under these conditions and we used the definitions (4)–(6). According to our estimates, the measured values were somewhat higher than the detection efficiency of fast neutrons that would be measured under ideal conditions. However, in real conditions where the detection of hidden nuclear materials would be carried out, the intrinsic efficiency and sensitivity of detection systems would likely correspond to our results.

An important fact should be noted. The sensitivity to fast neutrons of the proposed multi-layer ZEBRA-detectors of dimensions 100 × 100 × 41 mm is two times higher than the sensitivity of detectors based on heavy oxide scintillator single crystals, and is comparable to the sensitivity of a typical ^{3}He counter with a size and weight that is more than 10 times larger.

As can be seen from Table 2, within experimental errors the intrinsic detection efficiency of fast neutrons depends only on the total thickness of the active and passive layers of the detector, and it is only weakly dependent upon the area of the plates over a broad range. The detection efficiency reaches 40%–50%, which means very high ability of ZEBRA-detectors to discover fissionable nuclear materials hidden in containers. The detection sensitivity for detectors of dimensions 100 × 100 × 41 mm^3 reaches the value of 51 cps/(nps × cm^{-2}). If we assume that the activity of 1 ng of "fresh" nuclide ^{252}Cf per unit solid angle is 2.314 × 10^3 nps ng^{-1} (see, for example, [38]), the flux of fast neutrons at a distance of 200 cm passing through a surface of area S, expressed in [cm^2] units, is equal to $0.058 \times S$ nps ng^{-1}. Hence, we obtain a convenient relationship between detector sensitivity η and the equivalent threshold $\eta_{^{252}Cf}$ of the counting rate for reliable recording of the ^{252}Cf source at the distance 2 m from the detector:

$$\eta_{^{252}Cf} \approx 0.058\eta. \tag{7}$$

For ZEBRA-detectors of dimensions not less than 100 × 100 × 41 mm^3 with sensitivity η above 50 cps/(nps × cm^{-2}), the equivalent threshold for detection of ^{252}Cf, calculated according to (7), is 2.9 cps/ng, which is greater than the generally accepted standard IEC 62244 [39] for portal monitors — sensitivity to fast neutrons should not be less than 2.5 cps/ng. Therefore, our ZEBRA-detectors can be considered as promising for the creation of a new generation of solid-state portal monitors as an alternative to stationary ^{3}He counters.

Comparative analysis of the results presented in Table 2 leads to two important conclusions. First, the intrinsic detection efficiency of fast neutrons obtained with multi-layer detectors with thickness comparable to characteristic dimensions of large and expensive single crystal heavy oxide scintillators (dimensions from ø40 × 80 mm and higher), is comparable to the latter, reaching 50%. Also, the sensitivity of these multi-layered detectors is several times higher as compared with detectors using single crystals and can be increased even more by enlarging the sensitive area of the detecting plates.

It should be noted that measurements of the detection efficiency of ZEBRA-detectors based on one and the same heavy oxide scintillation material are dependent upon: (i) the choice of the direction of irradiation, which can fall onto the multi-layer detector parallel or normal to the layers; (ii) the total thickness of the detector; (iii) the number and thickness of layers in the composite scintillator; and (iv) the height of the detector in direction of the output window (i.e., the distance between the outer boundaries of the detector and the photoreceiver). The optimum detector design allows the avoidance of losses in detection of neutrons. Studies of these aspects are the subject of continuing investigations.

6. Conclusions

In this work, we have carried out qualitative and quantitative studies on the effects of possible nuclear reactions (channels of interaction of neutrons with scintillator nuclei) upon the efficiency of fast neutron detection by heavy oxide single crystal detectors and multi-layer composite detectors. Our experiments have convincingly shown that the main role in fast neutron detection by heavy oxide single crystals like ZWO, CWO, BGO, GSO(Ce) etc. is played by the reaction of inelastic scattering of fast neutrons. Experiments on detectors with external moderators, as well as theoretical estimates, show that it is possible to improve intrinsic detection efficiency by involving additional mechanisms of resonance

Table 2
Intrinsic efficiency and sensitivity of fast neutron detection by single crystal detectors and multi-layer ZEBRA-detectors. The measurements were carried out in the counting mode. ^{239}Pu–Be (at distance 100 cm from detectors) and ^{252}Cf (at distances 65 cm, 100 cm and 125 cm from detectors) neutron sources were used. The measurement errors do not exceed a few per cent.

Detector type	Scintillator size, mm	Neutron flux, nps cm^{-2}	Count rate, cps	Sensitivity, η cps/nps cm^{-2}	Intrinsic efficiency, ε %
BGO single crystal	ø40 × 80	0.76	7.47	9.83	48
ZWO single crystal	ø45 × 73	0.76	8.63	11.35	54
GSO(Ce) single crystal	ø12 × 10	0.76	0.26	0.35	46
ZEBRA-BGO-1	40 × 40 × 41	3.85	24.64	6.40	40
ZEBRA-BGO-2	100 × 40 × 41	1.70	27.20	16.00	40
ZEBRA-BGO-3	100 × 100 × 41	1.08	43.20	40.00	40
ZEBRA-ZWO-1	40 × 40 × 41	3.85	27.10	7.04	44
ZEBRA-ZWO-2	100 × 40 × 41	1.70	19.38	11.40	45
ZEBRA-ZWO-3	100 × 100 × 41	1.08	49.68	46.00	46
ZEBRA-GSO(Ce)-1	40 × 40 × 41	3.85	30.03	7.80	49
ZEBRA-GSO(Ce)-2	100 × 40 × 41	1.70	33.32	19.60	50
ZEBRA-GSO(Ce)-3	100 × 100 × 41	1.08	55.08	51.00	51
^{3}He counter[a]	1000 × 160 × 50	N/A	21.00	48.00	3

[a]With an additional massive 1000 × 200 × 50 mm plastic moderator of weight about 10 kg.

scattering and radiative capture in the case when the scintillator material contains heavy nuclei with large scattering cross-sections for these reactions.

An optimum combination of inelastic and resonance scattering, as well as thermal neutron radiative capture (in the presence of such nuclei as ^{113}Cd, ^{155}Gd, ^{157}Gd) is possible in the developed multi-layer ZEBRA-detectors on the basis of heavy oxide composite scintillators. Despite a much lower amount of the active substance (i.e., the heavy oxide composite scintillator material) that detects neutrons in such detectors, fast neutron detection efficiency in such detectors reaches 40%–50%, which is practically comparable with detection efficiency of expensive and large-sized heavy oxide single crystals. At the same time, the detection sensitivity and detection thresholds of hidden special nuclear materials by ZEBRA-detectors are several times higher. With a sensitivity to fast neutrons of about 50 cps / (nps × cm^{-2}) and better, these detectors are comparable to ^{3}He counters, but have much smaller (by tens of times) size and weight.

An important distinction of the proposed physical approach from all the known ways to replace ^{3}He counters by solid-state or gas discharge detectors is that practically all these methods propose to replace ^{3}He by other media that detect satisfactorily only thermal neutrons (^{6}Li and ^{10}B technologies), i.e., the basis for detection of fast neutrons requires the use of massive plastic moderators. Without such external moderators, intrinsic fast neutron detection efficiency for these primarily thermal detectors is extremely low, and even with moderation, does not exceed a few percent (for fast neutron energies greater than ~1 MeV). In our approach, fast neutrons are detected directly by heavy oxide scintillators in the crystal itself or in a multi-layer composite detector, which ensures much higher detection efficiency – up to 40%–50% – with improved sensitivity of the detector to fast neutrons. As a consequence, the sensitivity of such detectors in detection of special nuclear materials, including those hidden in protective containers, will be substantially higher.

References

[1] A.N. Caruso, The physics of solid-state neutron detector materials and geometries, J. Phys.: Condens. Matter 22 (2010) 443201, 1-32, http://dx.doi.org/10.1088/0953-8984/22/44/443201.

[2] R.T. Kouzes, A.T. Lintereur, E.R. Siciliano, Progress in alternative neutron detection to address the helium-3 shortage, Nucl. Instrum. Methods Phys. Res. A 784 (2015) 172–175. http://dx.doi.org/10.1016/j.nima.2014.10.046.

[3] T. Kojima, M. Katagiri, N. Tsutsui, K. Imai, M. Matsubayashi, K. Sakasai, Neutron scintillators with high detection efficiency, Nucl. Instrum. Methods Phys. Res. A 529 (2004) 325–328.

[4] P. Peerani, A. Tomanin, S. Pozzi, J. Dolan, et al., Testing on novel neutron detectors as alternative to^{3}He for security applications, Nucl. Instrum. Methods Phys. Res. A 696 (2012) 110–120. http://dx.doi.org/10.1016/j.nima.2012.07.025.

[5] J.L. Lacy, A. Athanasiades, C.S. Martin, L. Sun, G.J. Vazquez-Flores, The evolution of neutron straw detector applications in homeland security, IEEE Trans. Nucl. Sci. 60 (2) (2013) 1140–1146.

[6] A. Alemberti, M. Battaglieri, E. Botta, R. de Vita, et al., SCINTILLA: A European project for the development of scintillation detectors and new technologies for nuclear security, https://arxiv.org/abs/1404.3563 [physics.ins-det] 2014; http://www.scintilla-project.eu.

[7] N.J. Cherepy, R.D. Sanner, P.R. Beck, E.L. Swanberg, et al., Bismuth- and lithium-loaded plastic scintillators for gamma and neutron detection, Nucl. Instrum. Methods Phys. Res. A 778 (2015) 126–132. http://dx.doi.org/10.1016/j.nima.2015.01.008.

[8] V.N. Marin, R.A. Sadykov, D.N. Trunov, V.S. Litvin, et al., A new type of thermal-neutron detector based on ZnS(Ag)/LiF scintillator and avalanche photodiodes, Tech. Phys. Lett. 41 (9) (2015) 912–914. http://dx.doi.org/10.1134/S1063785015090242.

[9] S. Lam, J. Fiala, M. Hackett, S. Motakef, A high-performance CLYC(Ce)-PVT composite for neutron and gamma detection, IEEE Trans. Nucl. Sci. 65 (1) (2018) 609–615.

[10] M. Flaska, S.D. Clarke, C.C. Lawrence, S.A. Pozzi, J.B. Czirr, L.B. Rees, Characterization of cadmium capture-gated detector for nuclear non-proliferation applications, in: 2010 IEEE Nuclear Science Symposium, Knoxville, TN, USA, 2010.

[11] I.A. Paweczak, J. Toke, E. Henry, M. Quinlan, H. Singh, W.U. Schroder, NSTAR – A capture gated plastic neutron detector, Nucl. Instrum. Methods Phys. Res. A 629 (2011) 230–238.

[12] Yi Liu, Yi-Gang Yang, Yang Tai, Zhi Zhang, A capture-gated fast neutron detection method, Chin. Phys. C 40 (7) (2016) 076201/1-8.

[13] N.Z. Galunov, N.L. Karavaeva, O.A. Tarasenko, Crystalline and composite scintillators for fast and thermal neutron detection, in: M. Korzhik, A. Gektin (Eds.), Engineering of Scintillation Materials and Radiation Technologies, in: Springer Proceedings in Physics, vol. 200, 2016, pp. 195–208. http://dx.doi.org/10.1007/978-3-319-68465-9_12.

[14] O. Hausser, M.A. Lone, T.K. Alexander, S.A. Kushneriuk, The prompt response of bismuth germanate and NaI(Tl) scintillation detectors to fast neutrons, Nucl. Instrum. Methods Phys. Res. A 213 (1983) 301–309.

[15] S. Kubota, T. Motobayashi, M. Ogiwara, H. Murakami, Y. Ando, J. Ruan, S. Shirato, Response of BaF_2, BaF_2-plastic, and BGO scintillators to neutrons with energies between 15 and 45 MeV, Nucl. Instrum. Methods Phys. Res. A 285 (1989) 436–440.

[16] M. Anelli, G. Battistoni, S. Bertolucci, C. Bini, et al., Measurement and simulation of the neutron response and detection efficiency of a Pb-scintillating fiber calorimeter, Nucl. Instrum. Methods Phys. Res. A 580 (2007) 368–372.

[17] V.D. Ryzhikov, B.V. Grinyov, G.M. Onyshchenko, L.A. Piven, O.K. Lysetska, L.L. Nagornaya, T. Pochet, The use of fast and thermal neutron detectors based on oxide scintillators in inspection systems for prevention of illegal transportation of radioactive substances, IEEE Trans. Nucl. Sci. 57 (5) (2010) 2747–2751.

[18] V.D. Ryzhikov, B.V. Grinyov, G.M. Onyshchenko, L.A. Piven, S. Naydenov, O.K. Lysetska, The highly efficient gamma-neutron detector for control of fissionable radioactive materials, Funct. Mater. 21 (3) (2014) 345–351.

[19] V.D. Ryzhikov, S.V. Naydenov, L.A. Piven, G.M. Onyshchenko, C.F. Smith, T. Pochet, Fast neutron detectors and portal monitors based on solid-state heavy-oxide scintillators, Radiat. Meas. 105 (2017) 17–25. http://dx.doi.org/10.1016/j.radmeas.2017.08.008.

[20] V. Ryzhikov, B. Grinyov, G. Onyshchenko, L. Piven, O. Lysetska, L. Nagornaya, High efficiency method of fast neutron detection by oxide scintillators for detection systems of fissionable radioactive substances, in: Proc. ANIMMA-2011 Conference, Ghent, Belgium, 2011. http://dx.doi.org/10.1109/ANIMMA.2011.6172929.

[21] V.D. Ryzhikov, S.V. Naydenov, G.M. Onyshchenko, T. Pochet, C.F. Smith, High eefficiency fast neutron detectors based on inorganic scintillators, in: Proc. 2014 IEEE NSS-MIC Conference, Seattle, WA, USA, 2014. http://dx.doi.org/10.1109/NSSMIC.2014.7431165.

[22] B. Grynyov, V. Ryzhikov, L. Nagornaya, G. Onishcenko, L. Piven, Method of detection of fast neutrons, US 8058624 B2, 2011.

[23] V. Ryzhikov, C. Smith, B. Grinyov, L. Piven, G. Onyshchenko, S. Naydenov, T. Pochet, Detection of gamma-neutron radiation by novel solid-state scintillation detectors, in: Proc. ANIMMA-2015 Conference, Lisbon, Portugal, 2015.
[24] V.D. Ryzhikov, S.V. Naydenov, G.M. Onyshchenko, L.A. Piven, V.S. Zvereva, T. Pochet, C.F. Smith, A new multilayer scintillation detector for detection of neutron gamma radiation, in: Proc. 2015 IEEE NSS-MIC Conference, San Diego, CA, USA, 2015.
[25] V.D. Ryzhikov, B.V. Grinyov, S.V. Naydenov, G.M. Onyshchenko, L.A. Piven, Method of registration of fast neutrons and combined detector based thereon, Patent Application of Ukraine #a201611057, 2016.
[26] V.D. Ryzhikov, S.V. Naydenov, G.M. Onyshchenko, L.A. Piven, T. Pochet, C.F. Smith, Fast neutron detectors based on solid-state single crystalline and multilayer composite scintillators, in: Proc. 2016 IEEE NSS-MIC Conference, Strasbourg, France, 2016.
[27] V.D. Ryzhikov, S.V. Naydenov, T. Pochet, G.M. Onyshchenko, L.A. Piven, C.F. Smith, Advanced multilayer composite heavy-oxide scintillator detectors for high efficiency fast neutron detection, in: Proc. ANIMMA-2017 Conference, Liege, Belgium, 2017.
[28] N.S. Bowden, P. Marleau, J.T. Steele, S. Mrowka, G. Aigeldinger, W. Mengesha, Improved fast neutron spectroscopy via detector segmentation, Nucl. Instrum. Methods Phys. Res. A 609 (2009) 32–37.
[29] Y.I. Chernukhin, A.A. Yudov, S.I. Streltsov, Fast-neutron heterogeneous scintillation detector with high discrimination of gamma background, Nucl. Energy Technol. 1 (2) (2015) 130–134.
[30] M. Mohsen, Monte Carlo simulation of a fast neutron counter for use in neutron radiography, Nucl. Instrum. Methods Phys. Res. A 788 (2015) 73–78.
[31] A. Akhiezer, I. Pomeranchuk, Certain Problems of Nuclear Theory, second ed., Gostekhizdat, Moscow, Leningrad, 1950 (in Russian).
[32] J.M. Blatt, V.F. Weisskopf, Theoretical Nuclear Physics, Springer, New York, 1979.
[33] K.H. Beckurts, K. Wirtz, Neutron Physics, Springer-Verlag, Berlin, Heidelberg, 1964.
[34] Japan Atomic Energy Agency, Nuclear Data Center, JENDL (Japanese Evaluated Nuclear Data Library), Japan, 2018. http://wwwndc.jaea.go.jp/jendl/j40/j40.html.
[35] IAEA, International Nuclear Information System, NuDat-2, Selected evaluated nuclear structure data, 2018, http://www.nndc.bnl.gov/nudat2/.
[36] A.I. Abramov, Yu.A. Kazanski, E.S. Matusevich, Foundation of Experimental Methods in Nuclear Physics, second ed., Atomizdat, Moscow, 1977 (in Russian).
[37] S.D. Clarke, M.C. Hamel, A. Di Fulvio, S.A. Pozzi, Neutron and gamma-ray energy reconstruction for characterization of special nuclear material, Nucl. Eng. Technol. 49 (6) (2017) 1354–1357. http://dx.doi.org/10.1016/j.net.2017.06.005.
[38] R.T. Kouzes, J.R. Ely, A.T. Lintereur, D.L. Stephens, Neutron Detector Gamma Insensitivity Criteria, Technical Report PNNL-18903, Pacific Northwest National Laboratory, Richland, WA, USA, 2009.
[39] IEC/FDIS 62244 (2006-06), Installed radiation monitors for the detection of radioactive and special nuclear materials at national borders, 2006. http://www.iec.ch.